

# Ultra-fast Charge Migration Competes with Proton Transfer in the Early Chemistry of $\text{H}_2\text{O}^{+\bullet}$

Furong Wang, Uli Schmidhammer, Aurélien de La Lande and Mehran Mostafavi  
*Laboratoire de Chimie Physique, CNRS/Université Paris-Sud, Bât. 349, 91405 Orsay,  
France.*

## SUPPLEMENTARY INFORMATION

**Figure S1.** *Franck-Condon density-of-states for the electron transfer from  $\text{HSO}_4^-$  toward  $\text{H}_2\text{O}^{+\bullet}$ .*

**Figure S2:** *Electron transfer rates calculated by the Jortner-Bixon formalism for the electron transfer from  $\text{HSO}_4^-$  toward  $\text{H}_2\text{O}^{+\bullet}$*

## Theoretical estimates of electron transfer rates

### Non-adiabatic rate expression

For an electron-transfer reaction taking place in the electronic perturbative regime, the rate may be calculated with the Jortner-Bixon formulation of ET theory which is derived from the Fermi Golden Rule<sup>1</sup>

$$k_{JB} = \frac{2\pi}{\hbar} \frac{1}{\sqrt{4\pi\lambda_o k_B T}} \langle H_{DA}^2 \rangle \sum_{b \in inner} \langle \chi_0^i | \chi_b^f \rangle^2 \exp\left(-\frac{(\Delta G^\circ + \Delta E_{vib} + \lambda_o)^2}{4\lambda_o k_B T}\right) \quad (1)$$

$k_B$  is the Boltzmann constant,  $T$  is the temperature and  $\hbar$  is Planck's reduced constant.  $H_{DA}$  is the electronic coupling between the  $\{H_2O^{*+}; HSO_4^-\}$  and  $\{H_2O; HSO_4^-\}$  electronic states.  $\langle \chi_0^i | \chi_b^f \rangle^2$  is the Franck-Condon factor between the initial ground vibronic state and the final vibronic state. In the Jortner-Bixon theory the quantum description of the nuclear reorganization upon ET is preserved only for a subset of vibrational modes (the so-called inner-sphere).<sup>2</sup> These modes are those belonging to the redox partners *i.e.*  $H_2O^{*+}$  and  $HSO_4^-$ . The outer-sphere reorganization is estimated by the standard Marcus theory<sup>3</sup> *via* the introduction of the outer-sphere reorganization energy  $\lambda_o$ .  $-\Delta G^\circ$  is the ET driving force and  $\Delta E_{vib}$  is the difference of vibrational energy associated with each pair of initial and final vibronic states. The key parameters  $\Delta G^\circ$ ,  $\lambda_o$ ,  $H_{DA}$ ,  $\Delta E_{vib}$  and  $\langle \chi_0^i | \chi_b^f \rangle^2$  have been calculated with Density Functional theory. The calculations were carried out for a concentration of sulfuric acid of 14 mol.L<sup>-1</sup> which is close to the concentration for which the production of  $HSO_4^-$  is maximum (see Fig.2 of the main text).

- $\Delta G^\circ$  was estimated as  $\Delta G_{ox}(HSO_4^-) + \Delta G_{red}(H_2O^+) + 1/R$  where  $\Delta G_{ox}(HSO_4^-)$  and  $\Delta G_{red}(H_2O^+)$  are the free energy of oxidation and reduction of  $HSO_4^-$  and  $H_2O^{*+}$  respectively, and  $R$  is the center-to-center distance between the reactants. The first two terms were calculated at the DFT level with the Gaussian09 program<sup>4</sup>. The environment of redox partners was simulated with an implicit continuum model of static

dielectric constant ( $\epsilon_s$ ) of 102.3.  $\epsilon_s$  was determined by a linear interpolation between pure water and neat sulfuric acid, the static dielectric constant of which amounts to 78.6 and 110.0 at room temperature<sup>5</sup>. In DFT calculation the BHandHLYP functional<sup>6</sup> and the 6-311G\*\* basis set<sup>7,8</sup> were used. This functional was chosen because of recent benchmark calculations showing that this functional compared well with reference wave-function methods.<sup>9</sup> We found a redox potential of 2.7 V/NHE for the  $\text{HSO}_4^\cdot / \text{HSO}_4^-$  couple. This is in excellent agreement with the experimental value of 2.5 V/NHE<sup>10</sup>. For the water radical cation we remark that no stable geometry in which  $\text{H}_2\text{O}^{+\cdot}$  hydrogen bonded to another water molecule could be obtained. Such a finding was previously described in the literature.<sup>9</sup> The notion of redox potential for  $\text{H}_2\text{O}^{+\cdot}$  in water is therefore not well defined. To circumvent this difficulty geometry optimizations were first performed for  $\text{H}_2\text{O}^{+\cdot}$  and  $\text{H}_2\text{O}$  in the gas phase and single point calculations with the implicit continuum model were subsequently carried out. This procedure leads to a redox potential of 4.45 V/NHE for the  $\text{H}_2\text{O}^{+\cdot} / \text{H}_2\text{O}$  couple. In Ref. <sup>11</sup> the redox potential of  $\text{H}_2\text{O}^{+\cdot}$  was estimated to 4 V/NHE based on thermodynamic cycle, a value which is close to our theoretical estimate. The last term ( $1/R$ ) entering the calculation of the driving force reflects the direct interaction between the reactants.

- The outer-sphere reorganization energy  $\lambda_o$  was calculated with the expression derived

by Marcus: 
$$\lambda_o = \left( \frac{1}{2a_{\text{H}_2\text{O}^+}} + \frac{1}{2a_{\text{HSO}_4^-}} - 1/R \right) \left( \frac{1}{D_{op}} - \frac{1}{\epsilon_s} \right)$$
 where  $a_x$  is the radius of

reactant x and  $D_{op}$  is the optical constant of the medium<sup>3</sup>.  $D_{op}$  was taken as the square of the experimental refractive index of an sulfuric acid solution concentrated at 75%<sup>12</sup>. The radii were obtained from the "Volume" module of the program Gaussian09 that maps the space occupied by a molecule based on the spread of the electron

density calculated at the DFT level.  $a_{\text{H}_2\text{O}^+}$  and  $a_{\text{HSO}_4^-}$  were evaluated at 2.53 and 3.53

Å respectively. We verified that the non-adiabatic rates are not sensitive to few percent variations of the reactant radii.

- The Franck-Condon factors were calculated under the harmonic approximation with the molFC program<sup>13</sup>. molFC reads the frequency analysis output files produced by Gaussian09. It determines the displacements and mixing of normal modes upon ET.

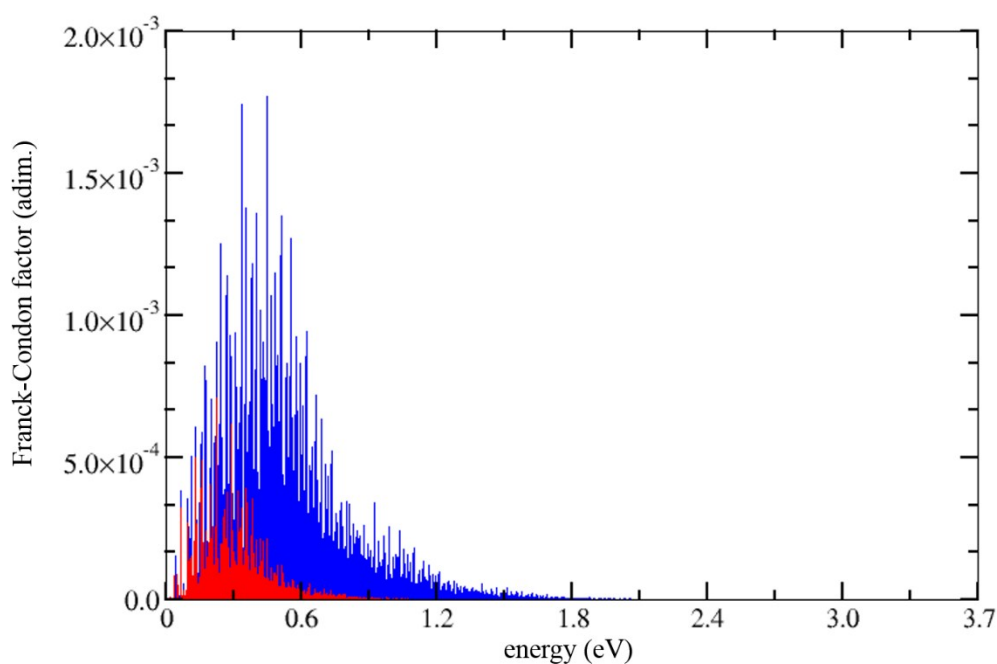


**Figure S1** | *Franck-Condon density-of-states arising from the inner-sphere: blue for  $\text{HSO}_4^-$  and  $\text{H}_2\text{O}^+$  and red for  $\text{DSO}_4^-$  to  $\text{D}_2\text{O}^+$ . The former allows a much wider range of energy to serve as reactive channel in the electron transfer process, hence faster rates in hydrogenated solutions.*

- The electronic coupling  $H_{DA}$  was calculated for a model of the  $\text{H}_2\text{O}^+ \cdots \text{HSO}_4^-$  ion pair at the constrained DFT level with the software deMon2k<sup>14,15</sup>. A series of geometries obtained by elongating the  $\text{H}_2\text{O}^+ \cdots \text{HSO}_4^-$  hydrogen bond was constructed. As expected the electronic coupling decays exponentially with the hydrogen bond length ( $R_{hb}$ ). The relationship relating the two quantities is:

$H_{DA} = H_{DA}^{eq} \exp \left[ -1.1811 (R_{hb} - R_{hb}^{eq}) \right]$  with  $H_{DA}^{eq} = 0.3249 eV$  with a linear regression coefficient of 0.991.

Figure S3 shows the evolution of the rate constant as a function of the hydrogen bond length ( $R_{hb}$ ). The origin corresponds to a close contact between the reactants, namely when a hydrogen bond of length 1.81 Å, as calculated by DFT, is formed between H<sub>2</sub>O and HSO<sub>4</sub><sup>-</sup>. The center-to-center distance  $R$  between reactants is defined as  $R = (R_{hb} - R_{hb}^{eq}) + a_{H_2O^+} + a_{HSO_4^-}$ . The evolution is non-monotonic and exhibits a maximum after 3 Å. This is easily understandable since each of the three parameters  $\Delta G^\circ$ ,  $\lambda_o$  and  $H_{DA}$  are sensitive to the separating distance. At very short distance the free energy of the reaction is positive because of the  $1/R$  term and a significant barrier to ET exists on the potential energy surface. As the distance between the partners increases  $\Delta G^\circ$  becomes more favorable and one reaches a point where  $-\Delta G^\circ \approx \lambda_o$ . However, at these distances the electronic coupling  $H_{DA}$  is weak and doesn't show ET in the sub-picosecond time domain. The rates are found to be slightly smaller in deuterated systems. The DFT-based estimate of  $\Delta G_{ox}(HSO_4^-) + \Delta G_{red}(H_2O^+)$  is -1.7eV. We repeated the calculations with the smaller value of -1.1eV that arise from the experimental<sup>10</sup>  $\Delta G_{ox}(HSO_4^-)$  (2.5eV) and the estimate  $\Delta G_{red}(H_2O^+)$  of -4eV proposed in Ref. <sup>11</sup>. We also find again that non-adiabatic ET cannot compete with a proton transfer taking place on the tens of femtoseconds time scale.

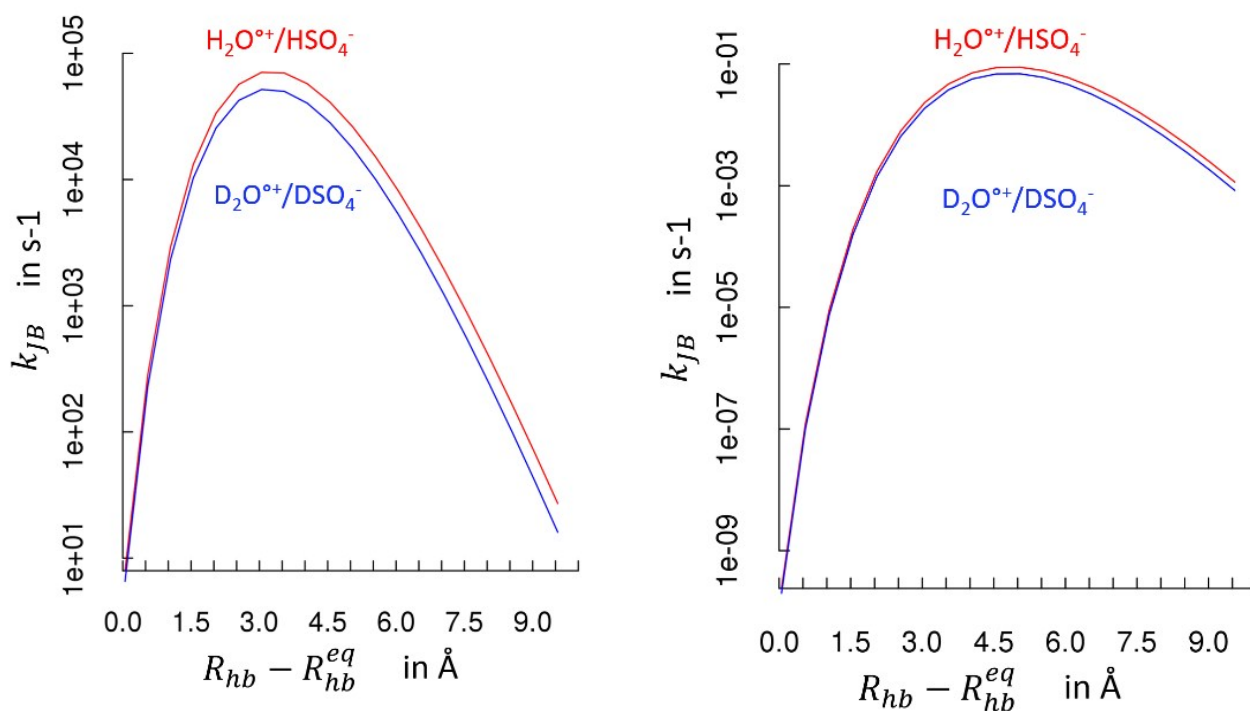


**Figure S2** | Electron transfer rates calculated by eq. 1. for the electron transfer from  $\text{HSO}_4^-$  to  $\text{H}_2\text{O}^+$  using either the DFT (Left) or experimental (Right) estimates of  $\Delta G_{\text{ox}}(\text{HSO}_4^-) + \Delta G_{\text{red}}(\text{H}_2\text{O}^+)$ .

#### Excess of energy in the electron cloud

The excess of energy present within the electron cloud after sudden ionization has been estimated as follow. We first determined the stationary electronic density of the  $\{\text{H}_2\text{O}; \text{HSO}_4^-\}$  system. The resulting Kohn-Sham determinant was subsequently used as a guess for the calculation of the  $\{\text{H}_2\text{O}^+; \text{HSO}_4^-\}$  system, *i.e.* after ionization. Molecular orbital permutations was operated to depopulate the highest MO localized on water and created a hole on water. The excess energy was then identified as the difference between the energies obtained from the KS determinant corresponding to the stationary electronic state of  $\{\text{H}_2\text{O}^+; \text{HSO}_4^-\}$  and with the KS determinant corresponding to the stationary electronic state of  $\{\text{H}_2\text{O}; \text{HSO}_4^-\}$ . Various exchange correlation energy functionals have been tested. The 6-311G\*\* basis set was used for all these calculations.<sup>7,8</sup> Excess energies of the order

of 7 eV were obtained with range-separated functionals (CAM-B3LYP<sup>16</sup>: 6.84 eV, M11<sup>17</sup>: 7.70 eV;  $\omega$ B97XD<sup>18</sup>: 7.12 eV). With the purely local BLYP<sup>19,20</sup> functional we obtained a value of 7.43 eV, while with global hybrids values of 6.76 eV and 8.10 eV were obtained with BHandHLYP<sup>6</sup> and B3LYP<sup>21</sup> respectively.

### *Simulation of ultrafast charge migration*

The electronic coupling between the  $\{ \text{H}_2\text{O}^+; \text{HSO}_4^- \}$  and  $\{ \text{H}_2\text{O}; \text{HSO}_4^* \}$  diabatic electronic states was found to amount to 0.36 eV, which is a very large value for which the non-adiabatic regime considered above is not applicable. Actually, given the strength of the interaction between the diabatic states, they should mix heavily. To simulate electronic dynamics at fixed nuclear positions real-time propagations of the electronic density was conducted at the DFT level with the NWCHEM module<sup>22,23</sup>. Two geometries were considered for which the hydrogen bond length was set to 1.81 Å (the equilibrium position of the pair  $\text{H}_2\text{O}/\text{HSO}_4^-$  before ionization) or 2.40 Å. We used the 6-311G\*\* basis set and the range separated CAM-B3LYP functional.<sup>16</sup> To assess the potential importance of diffuse functions, we compared the electronic spectra obtained by linear response TD-DFT with either the 6-311G\*\* or the 6-311++G\*\* basis sets. The difference of energy excitations with the two basis sets are well below 0.1eV, apart a few exceptions, for the fifteenth first excited states. The 6-311G\*\* thus offers a good quality/computation cost ration to describe the system. The DFT equations-of-motion were propagated with the Magnus scheme combined with a self-consistent extrapolation scheme<sup>23</sup>. An integration time-step of 3.6 as chosen. We verified that the total number of electrons was strictly conserved during the propagation. The initial electronic state was defined as follows. We first carried out an SCF calculation for the  $\text{H}_2\text{O}/\text{HSO}_4^-$  system. *i.e.* before ionization. Then an electron was removed from a valence molecular orbital of the water molecule and the TDDFT propagation was launched from this out-of-equilibrium electronic state.

**Table 1: Excited state energies, in eV calculated by Linear Response TD-DFT) with two basis sets. The electronic ground state is taken as energy reference.**

Excited state number	E (eV)	E (eV)	$\Delta E$ (eV)
	6-311++G**	6-311G**	
1	0.6195	0.5452	0.0743
2	0.9081	0.641	0.2671
3	1.0555	1.0434	0.0121
4	1.8074	1.8005	0.0069
5	1.9077	1.8683	0.0394
6	1.9487	1.9614	0.0127
7	2.7281	2.6711	0.057
8	2.9888	2.7018	0.287
9	4.7835	4.7475	0.036
10	5.6253	5.6168	0.0085
11	5.7888	5.6588	0.13
12	6.009	6.0766	0.0676
13	6.5827	6.5227	0.06
14	6.6827	6.7099	0.0272
15	6.7524	6.8187	0.0663



## REFERENCES

- 1 Bixon, M. & Jortner, J. Electron transfer - From isolated molecules to biomolecules. *Adv Chem Phys* **106**, 35-202, doi:DOI 10.1002/9780470141656.ch3 (1999).
- 2 Kestner, N. R., Logan, J. & Jortner, J. Thermal Electron-Transfer Reactions in Polar-Solvents. *J. Phys. Chem.* **78**, 2148-2166, doi:DOI 10.1021/j100614a017 (1974).
- 3 Marcus, R. A. & Sutin, N. Electron transfers in chemistry and biology. *Biochim. Biophys. Acta* **811**, 265-322, doi:[http://dx.doi.org/10.1016/0304-4173\(85\)90014-X](http://dx.doi.org/10.1016/0304-4173(85)90014-X) (1985).
- 4 Gaussian 09 (Gaussian, Inc., Wallingford, CT, USA, 2009).
- 5 Kliore, A. J., Elachi, C., Patel, I. R. & Cimino, J. B. Liquid content of the lower clouds of venus as determined from mariner 10 radio occultation. *Icarus* **37**, 51-72, doi:[http://dx.doi.org/10.1016/0019-1035\(79\)90115-5](http://dx.doi.org/10.1016/0019-1035(79)90115-5) (1979).
- 6 Becke, A. D. A new mixing of Hartree-Fock and local density-functional theories. *J. Chem. Phys.* **98**, 1372-1377, doi:doi:<http://dx.doi.org/10.1063/1.464304> (1993).
- 7 McLean, A. D. & Chandler, G. S. Contracted Gaussian basis sets for molecular calculations. I. Second row atoms, Z=11-18. *J. Chem. Phys.* **72**, 5639-5648, doi:doi:<http://dx.doi.org/10.1063/1.438980> (1980).
- 8 Petersson, G. A. & Al-Laham, M. A. A complete basis set model chemistry. II. Open-shell systems and the total energies of the first-row atoms. *J. Chem. Phys.* **94**, 6081-6090, doi:doi:<http://dx.doi.org/10.1063/1.460447> (1991).
- 9 Svoboda, O., Hollas, D., Oncak, M. & Slavicek, P. Reaction selectivity in an ionized water dimer: nonadiabatic ab initio dynamics simulations. *Phys. Chem. Chem. Phys.* **15**, 11531-11542, doi:10.1039/c3cp51440d (2013).
- 10 Neta, P., Huie, R. E. & Ross, A. B. Rate Constants for Reactions of Inorganic Radicals in Aqueous Solution. *J. Phys. Chem. Ref. Data* **17**, 1027-1284, doi:doi:<http://dx.doi.org/10.1063/1.555808> (1988).
- 11 Ma, J., Schmidhammer, U., Pernot, P. & Mostafavi, M. Reactivity of the Strongest Oxidizing Species in Aqueous Solutions: The Short-Lived Radical Cation H<sub>2</sub>O<sup>•+</sup>. *J. Phys. Chem. Lett.* **5**, 258-261, doi:10.1021/jz402411x (2014).
- 12 Palmer, K. F. & Williams, D. Optical Constants of Sulfuric Acid; Application to the Clouds of Venus? *Appl. Opt.* **14**, 208-219, doi:10.1364/ao.14.000208 (1975).
- 13 Raffaele, B., Amedeo, C. & Andrea, P. Franck-Condon factors—Computational approaches and recent developments. *Can. J. Chem.* **91**, 495-504, doi:doi:10.1139/cjc-2012-0518 (2013).
- 14 deMon2k Version 5 (Mexico City, 2016).
- 15 Řezáč, J., Lévy, B., Demachy, I. & de la Lande, A. Robust and Efficient Constrained DFT Molecular Dynamics Approach for Biochemical Modeling. *J. Chem. Theor. Comput.* **8**, 418-427, doi:10.1021/ct200570u (2012).
- 16 Yanai, T., Tew, D. P. & Handy, N. C. A new hybrid exchange-correlation functional using the Coulomb-attenuating method (CAM-B3LYP). *Chem. Phys. Lett.* **393**, 51-57, doi:<http://dx.doi.org/10.1016/j.cplett.2004.06.011> (2004).
- 17 Peverati, R. & Truhlar, D. G. Improving the Accuracy of Hybrid Meta-GGA Density Functionals by Range Separation. *J. Phys. Chem. Lett.* **2**, 2810-2817, doi:10.1021/jz201170d (2011).
- 18 Chai, J.-D. & Head-Gordon, M. Long-range corrected hybrid density functionals with damped atom-atom dispersion corrections. *Phys. Chem. Chem. Phys.* **10**, 6615-6620, doi:10.1039/b810189b (2008).
- 19 Becke, A. D. Density-functional exchange-energy approximation with correct asymptotic behavior. *Phys. Rev. A* **38**, 3098-3100 (1988).
- 20 Lee, C., Yang, W. & Parr, R. G. Development of the Colle-Salvetti correlation-energy formula into a functional of the electron density. *Physical Review B* **37**, 785-789 (1988).

- 21 Becke, A. D. Density-functional thermochemistry. III. The role of exact exchange. *J. Chem. Phys.* **98**, 5648-5652, doi:doi:<http://dx.doi.org/10.1063/1.464913> (1993).
- 22 Valiev, M. *et al.* NWChem: A comprehensive and scalable open-source solution for large scale molecular simulations. *Comput. Phys. Commun.* **181**, 1477-1489, doi:<http://dx.doi.org/10.1016/j.cpc.2010.04.018> (2010).
- 23 Lopata, K. & Govind, N. Modeling Fast Electron Dynamics with Real-Time Time-Dependent Density Functional Theory: Application to Small Molecules and Chromophores. *J. Chem. Theor. Comput.* **7**, 1344-1355, doi:10.1021/ct200137z (2011).